Materials Research Express

CrossMark

PAPER

The effect of BaF$_2$ concentration and particle size distribution on the luminescence efficiency of YAG:Ce^{3+} phosphors

D Valiev[1] , T Han[2], S Stepanov[1], V Vaganov[1] and V Paygin[1]

1   National Research Tomsk Polytechnic University, Lenin Avenue 30, 634050 Tomsk, Russia
2   Research Institute for New Materials Technology, Chongqing University of Arts and Sciences, Chongqing 402160, People's Republic of China

E-mail: dtdamirka@gmail.com

Abstract

Y$_3$Al$_5$O$_{12}$ (YAG) phosphor powders doped with Ce^{3+} concentration were synthesized by the solid-state reaction method with different of BaF$_2$ flux concentration. Morphological characterization, photoluminescent properties and decay characteristics of YAG phosphor powders were studied. It was shown that BaF$_2$ directly influenced on particle size distribution of YAG:Ce^{3+} phosphor. It is necessary to have both large particles agglomerates (size more than 40 μm) and small one (size less than 4 μm) to obtain high energy efficiency in polydisperse YAG:Ce^{3+} phosphors. It was evidenced, that the effect of both large and small agglomerates on energy efficiency is observed. The luminescence decay time for all investigated samples is significantly different in the spectral range 500 and 700 nm from $\tau \sim$ 60 to 80 ns, respectively.

1. Introduction

In past decade, light-emitting diodes (LED) are the most effective solid-state light sources [1]. Most commercially available white LEDs as rule consist of an InGaN blue LEDs combine with an Y$_3$Al$_5$O$_{12}$: Ce^{3+} (YAG: Ce^{3+}) yellow phosphor [2]. Generally, the magnitude of the physical limitation of the light yield for a white light LED is determined by the conversion of phosphor emission into a visible light [3]. Therefore, to enhance phosphor efficiency is one of the main directions of light sources development, resource efficiency, and creating a comfortable light environment, using different physical and chemical approaches for phosphor manufacturing.

Inorganic phosphors used by most manufacturers are yttrium-aluminum garnet doped with trivalent cerium ions (YAG: Ce^{3+}) synthesized with different methods. The luminescence spectrum of YAG:Ce^{3+} phosphors is characterized by a maximum wavelength in the spectral range of 530–560 nm due to emission from the 5d level to the ground state 4f energy level of Ce^{3+} [4]. The most common method for the commercial manufacturing of YAG phosphors is the solid-state reaction method (SSR) [5, 6]. However, for the phosphors preparation using SSR methods is required a sufficiently long treatment at high temperatures (over 1500 °C). The sintering process can be done in air, in an atmosphere of N$_2$/H$_2$, N$_2$/CO gas mixture [7]. This leads to partial sintering of the phosphor powder, and, consequently, it is necessary to grind the resulting mixture again. Different kinds of sintering fluxes are used to overcome the shortcomings of the SSR method [8, 9]. Fluoride type flux materials such as MgF$_2$, CaF$_2$, SrF$_2$, BaF$_2$, AlF$_3$ are efficient in the preparation of phosphor powders with garnet structures [10, 11]. Fluxes additions have a positive influence on the ion diffusions, crystallization process as well as on the formation of YAG host with good crystallinity in the SSR method [11–15].

The introduction of BaF$_2$ flux into the synthesis process is the most common approach in SSR route [15, 16]. The effect of flux can be derived from YAG single crystal growth [17]. In [10] it was shown the effect of BaF$_2$ on synthesized powder morphology of YAG:Ce^{3+} phosphor. The authors succeeded in achieving a high degree of particles size homogeneity when BaF$_2$ was 5 wt%. In addition, the grains had a spherical shape. The particle size of phosphors was 10–25 μm. In [18] also was demonstrated the effect of concentrations of the BaF$_2$ flux (3, 6, 9,

12, 15 wt%) on the morphology, crystal structure of TAG:Ce^{3+} phosphor with garnet structure. Particle sizes of phosphors with the addition of BaF$_2$ had a micron size and spherical shape, regardless of the BaF$_2$ concentration. The morphologies of the phosphor powders become spherical when the addition amount of the BaF$_2$ flux was increased. Authors have shown that when the BaF$_2$ concentration increase the particle size of phosphorus enhanced, without changes in the crystalline structure of TAG:Ce^{3+} phosphor. However, the phosphor powders prepared from the spray solution without the BaF$_2$ flux had irregular morphologies and aggregated structure. The usage of BaF$_2$ flux decreases of phosphor synthesis temperature, which as a result can significantly reduce power consumption and cost of phosphors production [18, 19]. The addition of flux creates wetted microdomains, which will improve mass diffusion and accelerate solid-state reactions [20].

Another important peculiarity flux using is the effect of BaF$_2$ on luminescent properties of YAG phosphor powders. In [10] the concentration of BaF$_2$ changed in the wide region from 3 to 15 wt%. The maximum photoluminescence intensity of the YAG:Ce^{3+} phosphor powders was observed for 9 wt% of BaF$_2$ concentration. It was demonstrated that the excitation peaks position of YAG:Ce^{3+} phosphor does not change with increasing concentration of BaF$_2$ [9]. This indicates that flux is chemically neutral and strong influence on optical properties of the initial powder particles of YAG: Ce phosphor. The high luminescence intensity for YAG:Ce^{3+} with 5 wt% BaF$_2$ phosphor was recorded.

Despite numerous studies the effect of BaF$_2$ flux on morphology and luminescent properties of YAG:Ce phosphor, we were not able to obtain information about direct investigations devoted to the effect of flux on luminescence decay kinetics of YAG:Ce^{3+} phosphor. Also, the effect of low BaF$_2$ flux concentrations with slight changes from 0.05 to 0.15 wt% and particle size distribution on the luminescence efficiency of YAG:Ce^{3+} phosphor has not been studied yet.

In this work, YAG:0.06Ce^{3+}, xBaF$_2$ powders (x = 0; 0.05; 0.075; 0.1; 0.125; 0.15 wt%) were synthesized by the solid-state reaction in order to determine the effect of BaF$_2$ flux doping and distribution of particle sizes on the luminescent and decay time properties. The study examined the preparation technique, the morphological characterization, luminescent properties, and decay characteristics.

2. Materials and methods

Phosphor powders were synthesized by high-temperature solid-state reaction method under reducing atmosphere. The preparation with this method requires repeated cycles of heating processes at high temperature up to 1600 °C to reinforce the interdiffusion and achieve a uniform single phase and homogeneity of the alloy. All reagents were a chemically pure Al$_2$O$_3$ (99.99%), Y$_2$O$_3$ (99.99%), CeO$_2$ (99.99%), and BaF$_2$ flux. The procedure used for the synthesis of YAG: 0.06 wt% Ce^{3+} + xBaF$_2$ (x = 0; 0.05; 0.075; 0.1; 0.125; 0.15 wt%) phosphor powders are presented in different steps. All of the initial materials were mixed in the desired ratio with the additional amount of BaF$_2$ used as flux material with different concentration. A single phase YAG:Ce^{3+} phosphor was obtained at 1500 °C [21].
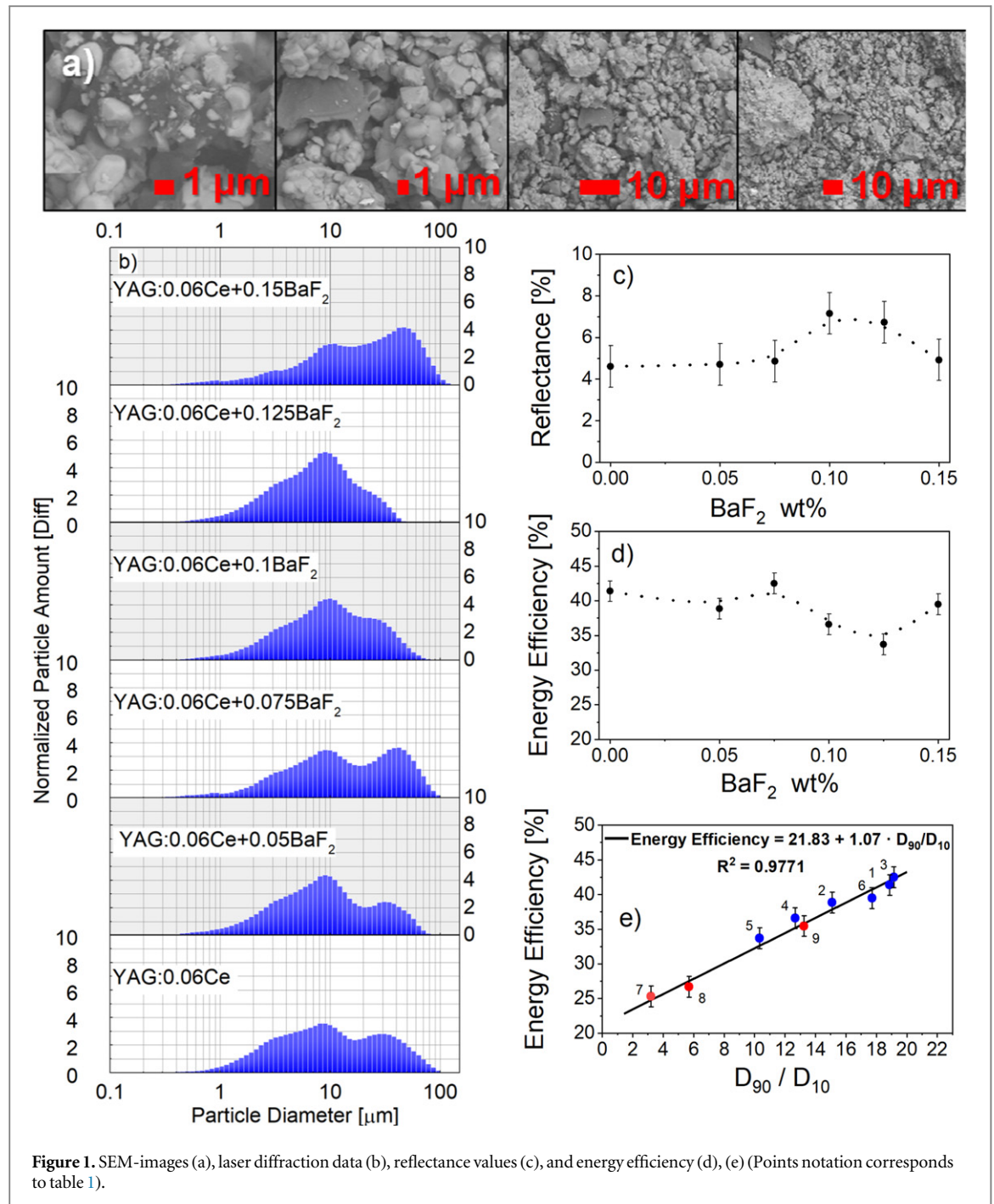
The obtained phosphor powders were characterized by Scanning Electron Microscopy (SEM) using a JSM-7500FA microscope (JEOL, Japan). The particle size analysis was conducted using a SALD-7101 Shimadzu laser particle size analyzer (Japan). The optical reflectance spectra of the sintered phosphors were measured by a LOMO-PHOTONICS SF-256UVI spectrophotometer (Russia) in the wavelength range of 300–1100 nm. Integrated photoluminescence (PL) spectra were acquired on an AvaSpec-3648 optical fiber spectrometer in 400–800 nm spectral range. An LED chip in pulse mode was used as excitation source for PL measurements (λ = 452 nm, FWHM is 10 nm, t$_{1/2}$ ∼ 15 ns). The photoluminescence decay kinetics was recorded with a photomultiplier tube Hamamatsu 10720–20 using a MDR-204 monochromator and a DPO3034 Tektronix (300 MHz) digital oscilloscope. The spectral power distribution of the total radiant flux of the PL spectra was measured by using an integrating sphere that was connected to a CCD detector (AvaSpec-3648) excited by an LED chip with following parameters: λ = 447 nm, FWHM 20 nm, 16 mW · cm^{-2} irradiance.

3. Results and discussion

3.1. Phosphor characterization
SEM images analysis of all investigated phosphors shows that YAG: 0.06Ce powders with different BaF$_2$ flux concentrations clearly consist of irregular shape and highly aggregated particles (figure 1(a)). According to the laser diffraction data, the particles have sizes from 1 to 100 μm (figure 1(b)).

The results of phosphors reflection data at the excitation band (λ = 447 nm) change from 4 to 8% (figure 1(c)). An estimate of the luminescence energy efficiency for all synthesized samples with a variable BaF$_2$ flux concentration under identical conditions show in figure 1(d). It is found that the energy efficiency decreases

Figure 1. SEM-images (a), laser diffraction data (b), reflectance values (c), and energy efficiency (d), (e) (Points notation corresponds to table 1).

with an increase of the reflectance and varies from 33% to 42%. Also reducing the sample reflection of the main absorption band at 450 nm is observed (figure 1(c)).

The particle size distribution for all investigated phosphors and additional data for YAG:Ce^{3+} phosphors with 10 wt% BaF_2 flux investigated earlier in [5] are presented in table 1. We did not find a direct correlation between energy efficiency and particle agglomerate sizes of phosphor powders for D_{10}, D_{50}, and D_{90}. However, from figures 1(a) and (d), it is evident that to obtain high energy efficiency of polydisperse phosphors it is necessary to have both large particles agglomerates (size more than 40 μm) and the small one (size less than 4 μm). In order to take into account the effect of both large and small agglomerates on energy efficiency. We analyzed the dependence of energy efficiency from the D_{90}/D_{10} ratio. The linear dependence of the energy efficiency of the YAG:Ce^{3+} with BaF_2 phosphor on the dimensions ratio of the total size distribution of 10 and 90 mass% (D_{90}/D_{10}) powder was obtained. The data analysis is presented in figure 1(e).

It should be noted, that an increase of BaF_2 concentration leads to a decrease in energy efficiency approximately on 15% of phosphor at a constant cerium concentration. Such effect was observed for YAG:Ce^{3+} phosphor doped with 10 wt% BaF_2 flux compared to YAG: 0.06Ce phosphor without flux (table 1, figure 1(e)).

Table 1. Particle size distribution and energy efficiency of YAG:Ce^{3+} phosphor powders.

	Phosphor powder	D_{10} [μm]	D_{50} [μm]	D_{90} [μm]	Energy efficiency [%]	D_{90}/D_{10}
1	YAG:0.06Ce	2.15	8.99	40.63	41.36	18.88
2	YAG:0.06Ce + 0.05BaF$_2$	2.21	8.59	33.39	38.83	15.10
3	YAG:0.06Ce + 0.075BaF$_2$	2.56	12.04	48.95	42.50	19.15
4	YAG:0.06Ce + 0.1BaF$_2$	2.40	9.21	30.51	36.60	12.67
5	YAG:0.06Ce + 0.125BaF$_2$	1.99	7.23	20.60	33.72	10.33
6	YAG:0.06Ce + 0.15BaF$_2$	3.60	21.80	63.73	39.50	17.72
7	YAG:0.06Ce + 10BaF$_2$ [5]	3.19	13.10	10.23	25.30	3.21
8	YAG:0.04Ce + 10BaF$_2$ [5]	3.50	8.63	19.95	26.70	5.70
9	YAG:0.02Ce + 10BaF$_2$ [5]	3.17	12.77	42.04	35.46	13.25

$^{*}D_{10}$, D_{50} and D_{90} are the particle sizes corresponding to a cumulative distribution of 10, 50 and 90 mass% of the powder, respectively. The D50 value corresponds to the median diameter.
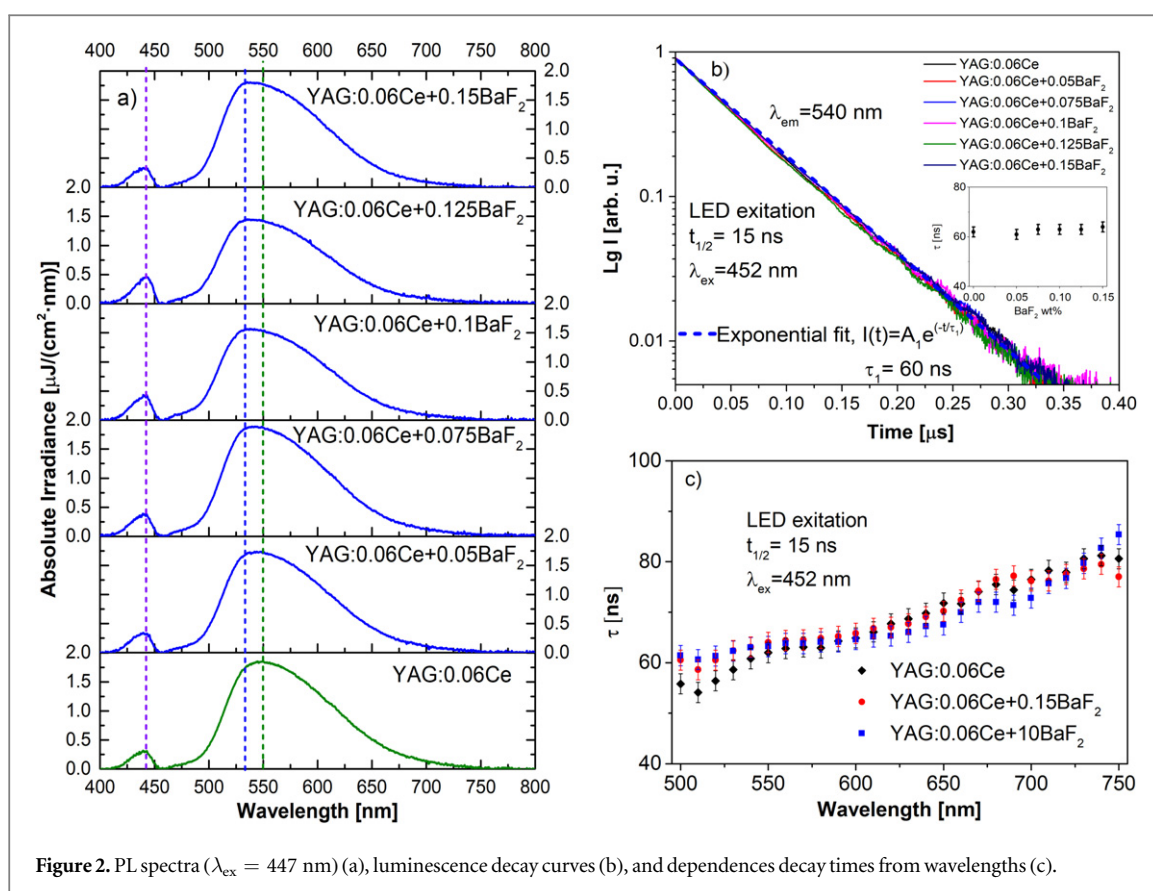
Figure 2. PL spectra ($\lambda_{ex} = 447$ nm) (a), luminescence decay curves (b), and dependences decay times from wavelengths (c).

In contrast, a decrease of cerium concentration at a constant barium fluorite concentration leads to an increase in the energy efficiency and agglomerates with D_{90} particles size (table 1). Both these processes are satisfactorily described by the obtained dependence of the energy efficiency on the D_{90}/D_{10} ratio (figure 1(e)).

3.2. Photoluminescent characteristics and luminescence decay kinetics

There are two bands in the excitation spectra monitored for the luminescence band at $\lambda_{max} = 540$ nm with a maximum at 342 and 463 nm. The results are similar that were obtained in our previous work [5]. These bands were recorded both for YAG:0.06Ce with and without BaF$_2$ powders. The spectra show two excitation bands that are assigned to transitions between the 4 f lowest energy level to 5d splitted sublevels [22, 23].

The PL spectra of YAG:Ce^{3+} phosphor powders with and without BaF$_2$ under blue LED chip excitation ($\lambda_{ex} = 447$ nm) are not significantly different (figure 2(a)). There are two peaks at 440 nm and intense emission with a maximum at 550 nm in the luminescence spectrum of the YAG:Ce^{3+} phosphors without BaF$_2$ flux are recorded. However, when BaF$_2$ flux with different concentration is introduced into YAG:Ce^{3+} phosphor the PL spectra of the powders are changed. The shape and the luminescence band position with a maximum at 550 nm possibly depend on the spin–orbit split ground state of Ce^{3+} ions. The crystal field surrounding Ce^{3+} ions splits

the 5d level into a number of sublevels. The most intense emission corresponds to the transition from the 5d lowest sublevel to the two levels of the 4f-shell. The splitting of the 4f level into the $^2F_{5/2}$ and $^2F_{7/2}$ states leads to the doublet character of the Ce^{3+} emission ions [24].

The luminescence decay kinetics for all investigated powders excited by LED chip working in pulsed mode was studied. It was experimentally observed that at 540 nm, the luminescence decay kinetics practically does not change depending on the BaF_2 concentration (figure 2(b) inset). However, the luminescence decay kinetics for all investigated phosphors have is significantly different in the spectral ranges of 500–600 and 650–750 nm, respectively (figure 2(c)). In the 'green' spectral region, one component with decay time is $\tau \sim 60$ ns. The luminescence decay kinetics describes the monomolecular reaction law. The radiative transition in each center occurs independently of the state of others and determined only by their probability. Nevertheless, in the 'red' spectral range (650–750 nm) the decay time is $\tau \sim 80$ ns.

However, in [25] the effect of BaF_2 flux on luminescence decays kinetics of $BaSi_3Al_3O_4N_5:Eu^{2+}$ phosphor prepared by the solid-state reaction was shown. Authors illustrated that for emission band at 470 nm of phosphors with and without flux the luminescence decay kinetics approximated by single exponential law. The decay time is slightly longer in the phosphors produced with BaF_2 flux ($\tau \sim 950$ ns). This effect can be described by decreasing of defect concentration due to enhance the crystallinity. The similar effect for $BaMgAl_{10}O_{17}:Eu^{2+}$ phosphors with LiF flux addition was observed in [26]. The authors also have been demonstrated the effect of decay time increasing for phosphor with 10% LiF flux from 1.06 μs to 1.17 μs. The process of decay time increasing connected with defect structure and enhancing of BAM:Eu^{2+} phosphor particles diameter.

Despite this fact, in our experimental results the effect of BaF_2 flux with 0.15 wt% and 10 wt% concentration on luminescence decay kinetics of YAG:Ce phosphor does not observed. The decay time is similar for YAG:Ce^{3+} without BaF_2 flux.

4. Conclusion

The structural, morphological, and optical properties of YAG:Ce phosphor powders synthesized by the solid-state reaction method with variable concentration of BaF_2 flux have been studied. The influence of barium fluoride flux on the luminescent and decay characteristics was carried out.

It was shown that BaF_2 directly influenced on particle size distribution of YAG:Ce phosphor. The experimental results show that it is necessary to have both large particles agglomerates (size more than 40 μm) and the small one (size less than 4 μm) to obtain high energy efficiency in polydisperse YAG:Ce phosphors. It was demonstrated that the effect of both large and small agglomerates on energy efficiency is observed. The introduction of BaF_2 flux leads to an increase in luminescence intensity. The luminescence decay time for all investigated samples is significantly different in the spectral range between 500 and 700 nm from $\tau \sim 60$ to 80 ns, respectively.

Such effect of BaF_2 flux on morphological and luminescent properties can be used for effective phosphor synthesis. This phenomenon can ultimately be substantially beneficial when used phosphors in white LEDs.

Acknowledgments

ORCID iDs

D Valiev   https://orcid.org/0000-0001-6880-7642

References

[1] Yeh N, Ding T and Yeh P 2015 Light-emitting diodes light qualities and their corresponding scientific applications *Renewable and Sustainable Energy Rev.* **51** 55–61

[2] Meyer J and Tappe F 2015 Photoluminescent materials for solid-state lighting: state of the art and future challenges *Adv. Opt. Mater.* **3** 424–30

[3] Ye S, Xiao F, Pan Y X, Ma Y Y and Zhang Q Y 2010 Phosphors in phosphor-converted white light-emitting diodes: Recent advances in materials, techniques, and properties *Mater. Sci. and Engin.* R **71** 1–34

[4] Xia Z and Meijerink A 2017 Ce^{3+}-doped garnet phosphors: composition modification, luminescence properties, and applications *Chem. Society Rev.* **46** 275–99

[5] Valiev D, Han T, Vaganov V and Stepanov S 2018 The effect of Ce^{3+} concentration and heat treatment on the luminescence efficiency of YAG phosphor *J. Phys. Chem. Solid.* **116** 1–6

[6] Jang S, Choi Y H, Wu S, Lim T G and Yoo J S 2016 Material properties of the Ce^{3+}-doped garnet phosphor for a white LED application *J. Inf. Disp.* **17** 117–23

[7] Tucureanu V, Matei A and Avram A M 2015 Synthesis and characterization of YAG:Ce phosphors for white LEDs *Opto-Electron. Rev.* **23** 239–51

[8] Ohno K and Abe T 1994 The synthesis and particle growth mechanism of bright green phosphor YAG:Tb *J. Electrochem. Soc.* **141** 1252

[9] Shiqing X U, Liuzheng S, Ying Z, Haidong J, Shilong Z, Degang D, Huanping W and Baoling W 2009 Effect of fluxes on structure and luminescence properties of $Y_3Al_5O_{12}$:Ce^{3+} phosphors *J. Rare Earths* **27** 327–32

[10] Lee S H, Jung D S, Han J M, Koo H Y and Kang Y C 2009 Fine-sized $Y_3Al_5O_{12}$:Ce phosphor powders prepared by spray pyrolysis from the spray solution with barium fluoride flux *J. of Alloys and Compd.* **477** 776–9

[11] Chiang C-H, Liu T-H, Lin H-Y, Kuo H-Y and Chu S-Y 2013 Effects of flux additives on the characteristics of $Y_{2.95}Al_5O_{12}$:$0.05Ce^{3+}$ phosphor: particle growth mechanism and luminescence *J. App. Phys.* **114** 243517

[12] Won C W *et al* 2011 Efficient solid-state route for the preparation of spherical YAG:Ce phosphor particles *J. of Alloys and Compd.* **509** 2621–6

[13] Shiqing X U *et al* 2009 Effect of fluxes on structure and luminescence properties of $Y_3Al_5O_{12}$:Ce^{3+} phosphors *J. Rare Earths* **27** 327

[14] Kim H, Kim J, Han J S and Park K 2016 Effect of BaF_2 flux on the photoluminescence properties of $Y_{2.94}Al_5O_{12}$: $0.06Ce^{3+}$ phosphors for white LED applications *Journal of Ceramic Processing Research* **17** 405–8

[15] Song Z, Liao J, Ding X, Liu X and Liu Q 2013 Synthesis of YAG phosphor particles with excellent morphology by solid state reaction *J. Cryst. Growth* **365** 24–8

[16] Won H I *et al* 2011 Effect of metal halide fluxes on the microstructure and luminescence of $Y_3Al_5O_{12}$:Ce^{3+} phosphors *Mater. Chem. Phys.* **129** 955–60

[17] Roberts K J and Elwell D 1981 Crystal habit and surface morphology of flux grown yttrium aluminium garnet *J. Cryst. Growth* **53** 249–60

[18] Lee S H *et al* 2009 Effects of BaF_2 flux on the properties of yellow-light-emitting terbium aluminum garnet phosphor powders prepared by spray pyrolysis *Opt. Mater.* **31** 870–5

[19] Ohno K and Abe T 1986 Effect of BaF_2 on the synthesis of the single-phase cubic $Y_3Al_5O_{12}$:Tb *J. Electrochem. Soc.* **133** 638–43

[20] Won H I *et al* 2017 Effect of BaF_2 powder addition on the synthesis of YAG phosphor by mechanical method *Adv. Powder Tech.* **28** 50–4

[21] Wang L, Zhao F, Zhang M, Hou T, Li Z, Pan C and Huang H 2016 Preparation and photoluminescence properties of YAG:Ce^{3+} phosphors by a series of amines assisted co-precipitation method *J. of Alloys and Compd.* **661** 148–54

[22] Pan Y, Wu M and Su Q 2004 Comparative investigation on synthesis and photoluminescence of YAG:Ce phosphor *Mater. Sci. and Engin. B: Solid-State Mater. for Adv. Tech.* **106** 251–6

[23] Zorenko Y, Zorenko T, Gorbenko V V, Voznyak T, Savchyn V, Bilski P and Twardak A 2012 Peculiarities of luminescent and scintillation properties of YAG:Ce phosphor prepared in different crystalline forms *Opt. Mater.* **34** 1314–9

[24] Wiatrowska A, Keur W and Ronda C 2017 Single and multicomponent garnets nanoparticles-synthesis and luminescence *J. Lumin.* **189** 9–18

[25] Tang J *et al* 2013 Fine-sized $BaSi_3Al_3O_4N_5$:Eu^{2+} phosphors prepared by solid-state reaction using BaF_2 flux *J. Mater. Res.* **28** 2598–604

[26] Wang X, Li J, Shi P, Guan W and Zhang H 2015 High dispersibility and enhanced luminescence properties of $BaMgAl_{10}O_{17}$:Eu^{2+} phosphors derived from molten salt synthesis *Opt. Mater.* **46** 432–7